diffusion-fundamentals.org
The Open-Access Journal for the Basic Principles of Diffusion Theory, Experiment and Application

Velocity-Sensitised Magnetic Resonance Imaging of Foams

Kevin J. Bos, K. Gordon Wilson, Benedict Newling

UNB MRI Centre, Dept. of Physics, University of New Brunswick, Canada.

Corresponding author: Benedict Newling, Dept. of Physics, University of New Brunswick, PO Box 5500, NB E3B 5A3 Fredericton, Canada, E-Mail: bnewling@UNB.ca

Abstract

Although flowing foams are used in a variety of technologies, foam rheology is still incompletely understood. In this paper we demonstrate the use of a velocity-sensitised magnetic resonance imaging (MRI) sequence for the study of flowing foam. We employ a constant-time (pure phase encode) imaging technique, SPRITE, which is immune to geometrical distortions caused by the foam-induced magnetic field inhomogeneity. The sample magnetisation is prepared before the SPRITE imaging with the Cotts 13-interval motion-sensitisation sequence, which is also insensitive to the effects of the foam heterogeneity. We measure the development of a power-law velocity profile in the foam downstream of a Venturi constriction (in which the cross-section of the tube decreases by 89% in area) in a vertical, cylindrical pipe.

Keywords

foam, velocity, SPRITE, constant time, Cotts 13-interval

1. Introduction

Flowing foams have a wide range of applications, including foods processing, enhanced oil recovery, pipeline transport and cleaning. Unfortunately, although foam rheology is complicated and difficult to model [1,2,3], measurement of the velocity field in flowing foams is complicated by their optical opacity and delicacy. Magnetic resonance imaging is an obvious candidate for non-invasive measurements in optically opaque systems and there has been successful application of MRI methods to the study of foams [4,5]. However, heterogeneous materials, pose some challenges to MRI. The variation in magnetic susceptibility at the liquid/gas boundaries causes local gradients in the magnetic field, which can cause distortions in an MR image. We have chosen an MRI protocol which is particularly robust to the effects of inhomogeneous magnetic field in order to measure velocity maps in the vertical flow of a wet foam.

2. Methods and Materials

Foam was generated in a vertical, cylindrical glass pipe by bubbling sulphur hexafluoride, SF_6(g), through a micron sparger immersed in a foaming mixture of 1.5 g/L sodium dodecyl sulphate (SDS, Aldrich, Ontario, Canada) and 30 mL/L glycerol (also Aldrich) in distilled water. The rising foam passed through a Venturi constriction in which the pipe diameter changed from 17.3 to 5.6±0.1 mm and emptied into an open reservoir. As the foam collapsed, the foaming mixture was pumped back to the sparger vessel.

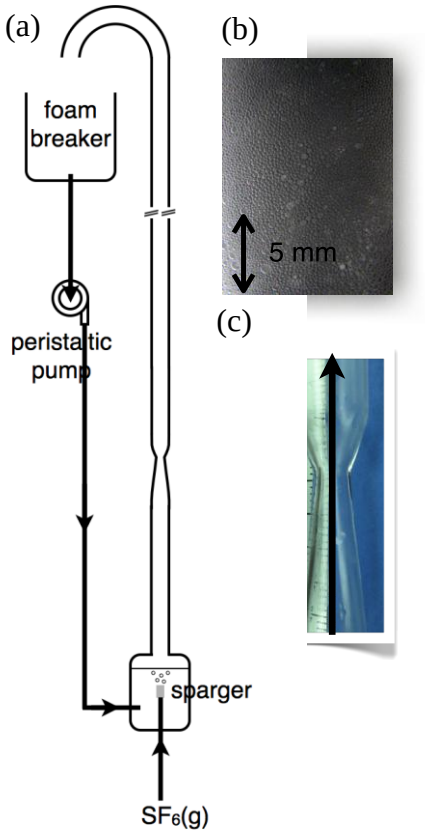

Fig. 1: (a) Glass column for foam production. The sparger is composed of sintered glass and the foam breaker is a wire basket, which can be rotated through the accumulating foam. The two insets show (b) a typical consistency of the foam produced at a gas flow rate of 250 ml/min and (c) the geometry of the constriction through which foam rises.

The apparatus is similar to that reported by Deshpande and Barigou [6] and the same basic design has been in use for foam research since the mid sixties (Fig. 1). In other work, the foam structure has been studied optically or using gamma rays, for example [6 and references therein].

In our measurements, the foam rose, as it was generated, up the bore of a 4.7 T magnet (Cryomagnetics, TN, USA) through a DSI 875 Litz RF coil (Doty Scientific, SC, USA) inside a homebuilt 3-axis set of gradient coil windings. The liquid was doped with $GdCl_3$ in order to reduce T_1 to 250 ms. T_1 was assessed using a saturation-recovery sequence because the foam is in constant motion.

Flow measurement was carried out using a Cotts-13-interval-prepared SPRITE sequence [7] (Fig. 2) executed by a Redstone console (Tecmag, TX, USA). SPRITE is a constant-time, purely phase-encoded imaging technique, which suffers no geometrical distortion, even in gravely inhomogeneous samples [8], because the susceptibility effects are the same at every data acquisition point. The 180º pulses (2 and 5) in the Cotts sequence somewhat refocus the effects of the inhomogeneous foam sample as far as the motion sensitisation is concerned [9].

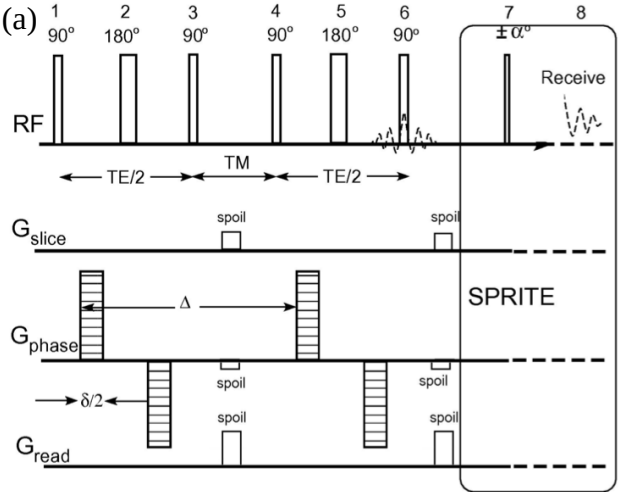

Fig. 2: (a) Pulse sequence diagram for the velocity-sensitised MRI measurement. The RF pulses 1-6 comprise the Cotts 13-interval preparation. Any of the SPRITE family of imaging sequences can follow: we employed SPRITE as described in [8], so that each prepared *k*-space trajectory was a single line of a Cartesian raster and therefore short in duration compared to T_1. (b) The phase cycle is shown in the table below [7].

(b)

1	2	3	4	5	6	7	8
X	Y	X	X	Y	X	X	X
Y	Y	X	Y	X	X	X	X
X	Y	X	X	Y	Y	Y	X
Y	Y	X	Y	X	Y	Y	X

The motion-sensitising interval Δ = 7.4 ms and the effective gradient pulse duration δ = 0.4 ms as drawn (although the gradient pulses were actually trapezoidal). In order to keep measurement times manageable, despite low proton density (foam/solution FID amplitudes at 31 µs, suggest 88% gas fraction), motion-sensitising gradient amplitudes of g_x = ±82.1 mT/m, g_y = ±47.3 mT/m, g_z = ±88.8 mT/m were employed in combination with a MATLAB (Mathworks, MA, USA) implementation of the Goldstein phase-unwrapping algorithm [10]. Images (32^2 points zero-filled to 64^2) took 3 minutes to acquire and the field of view was 60 x 46 mm^2, making the nominal size of each pixel 1.9 x 1.4 mm^2 (much larger than most bubbles in the foam). The α pulse (7) had a duration of 2 µs resulting in a tip angle of 8° and the phase-encoding interval which followed in the SPRITE imaging sequence was 170 µs.

3. Results

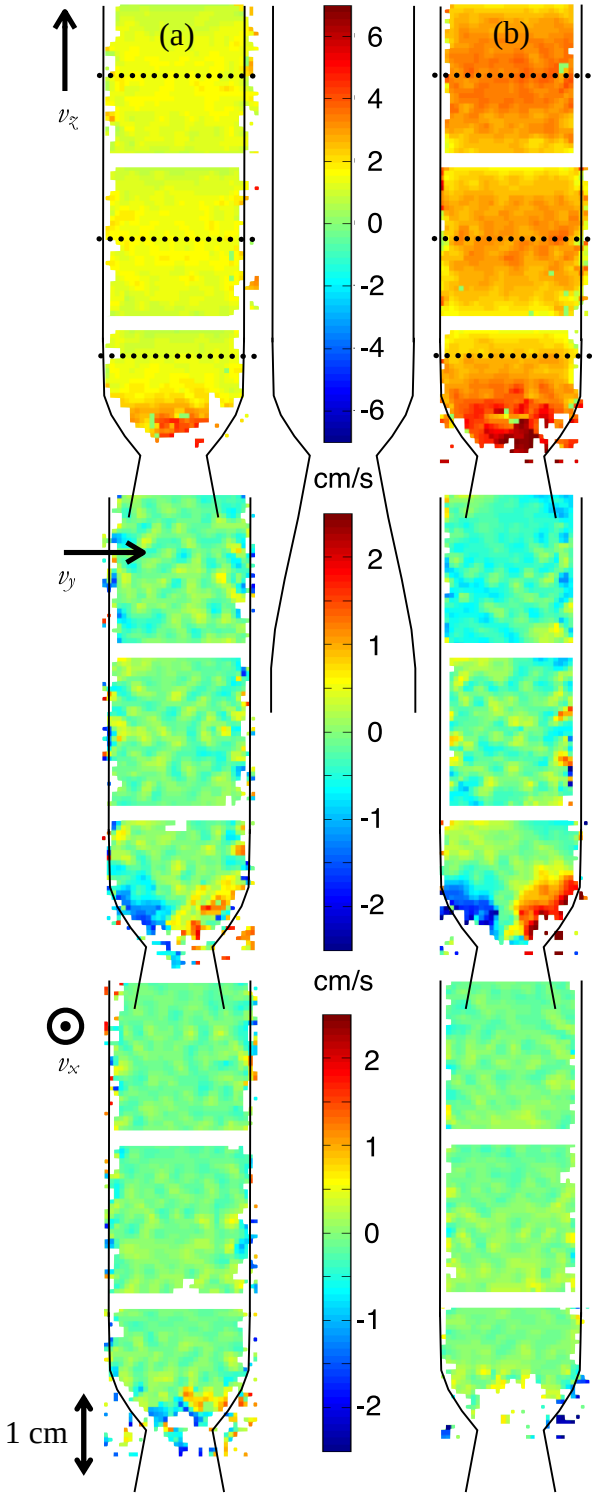

Fig. 3 shows maps of three components of velocity obtained at two different gas flow rates. The *z*-axis (with the marginally higher spatial resolution) is in the same direction as the polarising magnetic field (B_0), the *y*-axis is across the tube and the *x*-axis is out of the page.

Fig. 3: Velocity maps obtained using the pulse sequence of Fig. 2. Foam flows were generated with an SF_6(g) flow rate of (a) 250 ml/min and (b) 500 ml/min. The foam flows upwards (+*z*) through the constriction. The effects of the constriction upon the foam flow are limited in range. The dotted lines indicate the location of the profiles which appear in Fig. 4.

The flow of foam up the column shows plug-like behaviour and develops over less than a centimetre downstream of the constriction.

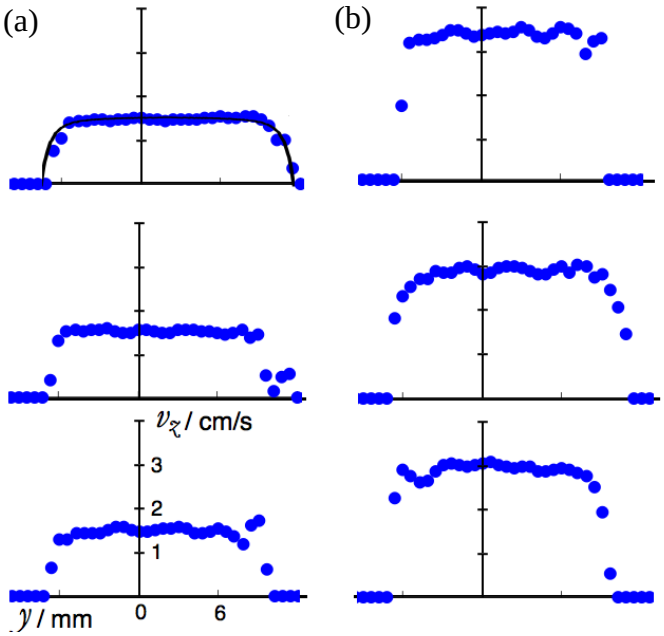

Fig. 4: Profiles of v_z taken at the locations indicated by dotted lines in Fig. 3. In the first column (a) are profiles with an SF_6(g) flow rate of 250 ml/min and in the second column (b) are the corresponding profiles with an SF_6(g) flow rate of 500 ml/min. The power-law model (solid line, top left) is described in the text.

Fig. 4 shows the developing v_z profiles measured from the velocity maps in figure 3 at the locations indicated by dotted lines. One sample model of power-law fluid flow

$$v_z(r) = \frac{r_{\max}^{\frac{1}{n}+1} - r^{\frac{1}{n}+1}}{\frac{1}{n}+1} \quad (1)$$

with r the distance from the tube centre, r_{max} the tube radius and n = 0.01, has been summed over the tube cross-section and is overlayed on the top left profile. Power-law models are used in the description of foam pipe flows [6].

4. Conclusions

Cotts-prepared SPRITE sequences are clearly capable and appropriate in the non-invasive study of foam flows. Foam generation has been sustained for up to 7 hours with no apparent degradation in foam production, which has allowed us sufficient time to also make these measurements in three dimensions. One complication is complexation of the Gd^{3+} ions by the SDS surfactant. This leads to a gradual increase in T_1 over several hours and some cloudiness. Additional surfactant restores the relaxation and optical behaviours, but also affects the foam properties. We plan, in future work, to use a pre-chelated contrast agent to avoid this problem. The three-dimensional velocimetry data will be part of a later report in which we map velocities using ^{1}H and ^{19}F measurements on the same flows. In this way we can compare the liquid and gas velocity fields in the foam. Some discrepancy is expected between the velocites of the two phases, because the liquid drains through the continuous phase at the same time as the foam rises up the column.

References

[1] Hutzler & Weaire, Colloids Surf. A 382 (2011) 3-7.
[2] Weaire, Curr. Opin. Colloid Int. Sci. 13 (2008) 171-176.
[3] Höhler & Cohen-Addad, J. Phys.: Condens. Matter 17 (2005) R1041-R1069.
[4] McCarthy, AIChE J. 36 (1990) 287-290.
[5] Rodts, Baudez & Coussot, Europhys. Lett. 69 (2005) 636-642.
[6] Deshpande & Barigou, Chem. Eng. Sci. 55 (2000) 4297.
[7] Li, Chen, Marble, Romero-Zerón, Newling & Balcom, J. Magn. Reson. 197 (2009) 1-8.
[8] Balcom, MacGregor, Beyea, Green, Armstrong & Bremner, J. Magn. Reson. A 123 (1996) 131.
[9] Cotts, Hoch, Sun & Marker, J. Magn. Reson. 83 (1989) 252.
[10] Spottiswood, MATLAB Central file exchange (2008); Ghiglia & Pritt "Two-Dimensional Phase Unwrapping", Wiley-Interscience,1998.

Acknowledgements

The authors would like to thank the National Science and Engineering Research Council (NSERC) of Canada for support and Rodney MacGregor and Brian Malcolm for indefatigable technical help.